Journal of Coordination Chemistry
Publication details, including instructions for authors and subscription information:
http://www.tandfonline.com/loi/gcoo20

Chalcone-derived thiosemicarbazones and their zinc(II) and gallium(III) complexes: spectral studies and antimicrobial activity

JEFERSON G. DA SILVA [a], CAMILA C.H. PERDIGÃO [a], NIVALDO L. SPEZIALI [b] & HELOISA BERALDO [a]

[a] Departamento de Química, Universidade Federal de Minas Gerais, Belo Horizonte, Brazil

[b] Departamento de Física, Universidade Federal de Minas Gerais, Belo Horizonte, Brazil

Accepted author version posted online: 11 Dec 2012.Published online: 29 Jan 2013.

To cite this article: JEFERSON G. DA SILVA, CAMILA C.H. PERDIGÃO, NIVALDO L. SPEZIALI & HELOISA BERALDO (2013) Chalcone-derived thiosemicarbazones and their zinc(II) and gallium(III) complexes: spectral studies and antimicrobial activity, Journal of Coordination Chemistry, 66:3, 385-401, DOI: 10.1080/00958972.2012.757762

To link to this article: http://dx.doi.org/10.1080/00958972.2012.757762

Journal of Coordination Chemistry
Vol. 66, No. 3, 10 February 2013, 385–401

Chalcone-derived thiosemicarbazones and their zinc(II) and gallium(III) complexes: spectral studies and antimicrobial activity

JEFERSON G. DA SILVA†, CAMILA C.H. PERDIGÃO†, NIVALDO L. SPEZIALI‡ and HELOISA BERALDO†*

†Departamento de Química, Universidade Federal de Minas Gerais, Belo Horizonte, Brazil; ‡Departamento de Física, Universidade Federal de Minas Gerais, Belo Horizonte, Brazil

(*Received 16 July 2012; in final from 16 October 2012*)

Chalcone-derived 3-phenyl-1-pyridin-2-ylprop-2-en-1-one thiosemicarbazone (HPyCTPh) (**1**), 3-(4-chlorophenyl)-1-pyridin-2-ylprop-2-en-1-one thiosemicarbazone (HPyCT4ClPh) (**2**), 3-(4-bromophenyl)-1-pyridin-2-ylprop-2-en-1-one thiosemicarbazone (HPyCT4BrPh) (**3**), and 3-(4-nitrophenyl-1-pyridin-2-ylprop-2-en-1-one thiosemicarbazone (HPyCT4NO_2Ph) (**4**) were obtained as well as their gallium(III) and zinc(II) complexes $[Ga(PyCTPh)_2]NO_3$ (**Ga1**), $[Ga(PyCT4ClPh)_2]NO_3$ (**Ga2**), $[Ga(PyCT4BrPh)_2]NO_3$ (**Ga3**), $[Ga(PyCT4NO_2Ph)_2]NO_3$ (**Ga4**), $[Zn(PyCTPh)_2]$ (**Zn1**), $[Zn(PyCT4ClPh)_2]$ (**Zn2**), $[Zn(PyCT4BrPh)_2]$ (**Zn3**), and $[Zn(PyCT4NO_2Ph)_2]$ (**Zn4**). The chalcones, thiosemicarbazones, and zinc(II) complexes were not active against *Pseudomonas aeruginosa*. The thiosemicarbazones proved to be more active than the parent chalcones against *Staphylococcus aureus* and *Candida albicans*. Coordination to zinc(II) resulted in activity improvement of most thiosemicarbazones against *S. aureus*. Coordination to gallium(III) significantly improved the antimicrobial activity of all thiosemicarbazones against the studied micro-organisms, suggesting this to be an effective strategy for antimicrobial activity enhancement.

Keywords: Chalcones; Thiosemicarbazone; Zinc(II) complexes; Gallium(III) complexes; Antimicrobial

1. Introduction

Chalcones (figure 1) are flavonoid compounds bearing the 1,3-diarylprop-2-en-1-one framework. They are the first isolable compounds from flavonoid biosynthesis in plants, with widespread distribution in fruits, vegetables, spices, tea, and soy [1]. These compounds exhibit a diverse range of pharmacological activities, presenting cytotoxic, antitumor, antiinflammatory, antiplasmodial, immunosuppressive, antimicrobial, and antioxidant properties [1,2].

Thiosemicarbazones also have wide pharmacological versatility and present cytotoxic, antitumor, antimalarial, antimicrobial, and antiviral properties [3]. In many cases, metal coordination leads to an improvement of thiosemicarbazones pharmacological activities and synergistic effects involving both metal and the thiosemicarbazone have been reported [3–7].

*Corresponding author. Email: hberaldo@ufmg.br

ISSN 0095-8972 print/ISSN 1029-0389 online © 2013 Taylor & Francis
http://dx.doi.org/10.1080/00958972.2012.757762

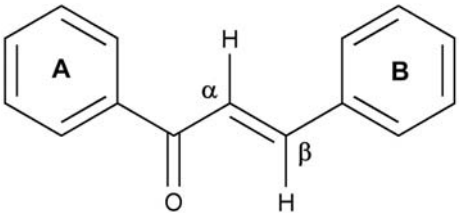

Figure 1. Structural framework of chalcones.

The mechanism of action of metal ions may involve binding to proteins, interaction with microbial membrane with changes in structure and permeability, and interaction with nucleic acids preventing microbial replication [8].

Zinc is the second most prevalent trace element, after iron, and is involved in structure and function of over 300 enzymes. Use of zinc as a nutritional supplement has become common in many countries [9]. Zinc salts, primarily zinc citrate, are widely used as antimicrobials. Zinc exhibits activity against oral *Streptococci*, particularly *Streptococcus mutans* [8]. Zinc supplementation shows beneficial effects against infectious diseases, especially diarrhea, and it has been shown that zinc supplementation can improve mucosal innate immunity through induction of antimicrobial peptide secretion from intestinal epithelial cells [10].

Gallium has efficacy in the treatment of disorders such as accelerated bone resorption, autoimmune diseases and allograft rejection, certain cancers, and infectious diseases [11]. The antimicrobial properties of gallium compounds have been demonstrated by other authors [11] and by our group [6,12,13].

The mechanism of antimicrobial action of gallium(III) is related to iron metabolism. Gallium(III) mimics iron(III) due to their similar charge-to-radius ratio. Hence, gallium(III)

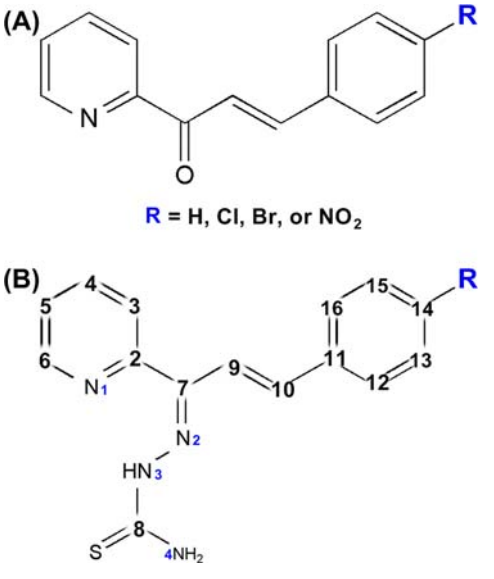

Figure 2. Structural representation for the chalcone precursors (A) and chalcone-derived thiosemicarbazones (B).

binds to ferric sites on transferrin and is acquired from transferrin by certain bacteria. However, unlike iron(III), it is not reducible to a divalent form under physiological conditions, which precludes its participation in crucial bacterial iron-dependent DNA-synthetic pathways [14]. Iron metabolism is a key vulnerability of infecting bacteria because organisms require iron for growth. A "Trojan horse" strategy that used gallium to disrupt bacterial iron metabolism has been reported in an experiment which showed that gallium inhibits *Pseudomonas aeruginosa* growth and biofilm formation and kills planktonic and biofilm bacteria *in vitro* [15].

Coordination of thiosemicarbazones to gallium(III) leads to improvement of antimicrobial properties [6,12,13] as well as their cytotoxic activity [16]. Combining a chalcone with a thiosemicarbazone framework could lead to compounds with interesting pharmacological profile. Thus, in the present work, a family of four chalcone-derived thiosemicarbazones were obtained (see figure 2) as well as their zinc(II) and gallium(III) complexes. The antimicrobial activities of the chalcone precursors (see figure 2) and the corresponding thiosemicarbazones and their zinc(II) and gallium(III) complexes were investigated.

2. Experimental

2.1. *Materials and measurements*

All chemicals were purchased from Aldrich and used without purification.

Elemental analyses were performed on a Perkin Elmer CHN 2400 analyzer. A YSI model 31 conductivity bridge was employed for molar conductivity measurements. High resolution mass spectra (HRMS) were recorded with a Shimadzu IT-TOF mass spectrometer. DMSO solutions of the compounds were diluted in methanol and applied in the electrospray ionization source for direct injection. Mass spectra were obtained in the full scan mode within the *m/z* 100–1000 range. Electronic spectra were obtained with an UV-2401PC – (P/N 206-82201) – Shimadzu. Infrared spectra were recorded on a Perkin Elmer FT-IR Spectrum GX spectrometer using KBr pellets. NMR spectra were obtained at room temperature with a Bruker DRX-400 Avance (200 MHz) spectrometer using deuterated dimethyl sulfoxide (DMSO-d_6) as the solvent and tetramethylsilane as internal reference. ^{1}H resonances were assigned on the basis of chemical shifts and multiplicities. The carbon type (C, CH) was determined by using distortionless enhancement by polarization transfer (DEPT 135) experiments. Single-crystal X-ray diffraction measurements were carried out on a GEMINI-Ultra diffractometer (LabCri-UFMG) using graphite-Enhance Source Mo $K\alpha$ radiation ($\lambda = 0.71073$ Å) at 120 K. Data collection, cell refinement results, and data reduction were performed using CRYSALISPRO software [17]. The semi-empirical from equivalents absorption correction method was applied [17]. Structures were solved by direct methods using SHELXS-97 [18]. Full-matrix least-squares refinement procedure on F^2 with anisotropic thermal parameters was carried out using SHELXL-97 [18]. Positional and anisotropic atomic displacement parameters were refined for all nonhydrogen atoms. Hydrogen atoms were placed geometrically and the positional parameters were refined using a riding model.

2.2. *Syntheses*

All compounds were obtained as described in scheme 1.

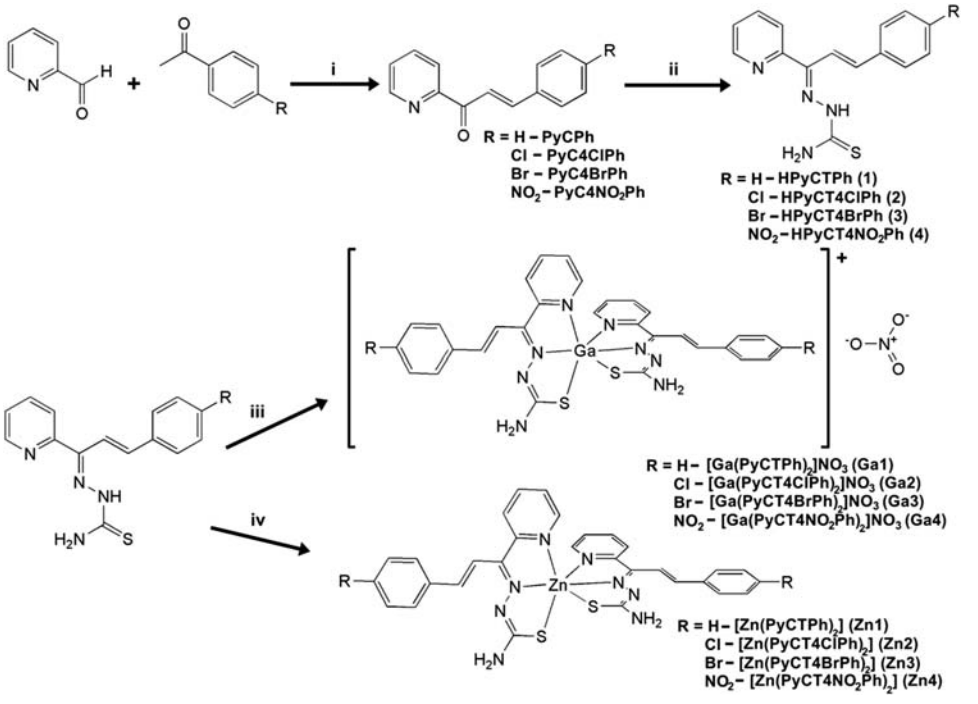

Scheme 1. General syntheses of chalcone-derived thiosemicarbazones (**1–4**) and their complexes (**Ga1**–**Ga4** and **Zn1**–**Zn4**). (i) NaOH 10%; (ii) thiosemicarbazide; (iii) gallium nitrate; (iv) zinc chloride; and sodium acetate.

2.2.1. Synthesis of the chalcone precursors: 3-phenyl-1-pyridin-2-ylprop-2-en-1-one (PyCPh), 3-(4-chlorophenyl)-1-pyridin-2-ylprop-2-en-1-one (PyC4ClPh), 3-(4-bromo phenyl)-1-pyridin-2-ylprop-2-en-1-one (PyC4BrPh), and 3-(4-nitrophenyl-1-pyridin-2-ylprop-2-en-1-one (PyC4NO$_2$Ph). The chalcones were obtained as previously reported [19]. A solution of NaOH 10% (7.5–12.5 mL) was added dropwise to a mixture of 2-acetylpyridine (10 mmol) and the desired aldehyde (10 mmol) in methanol (15 mL). The reaction mixture was kept under stirring for 1 h at room temperature. The resulting solids were filtered off, washed with water, and dried *in vacuo*.

2.2.2. Synthesis of the chalcone-derived thiosemicarbazones. To a mixture of the desired chalcone (4 mmol) and thiosemicarbazide (4 mmol) in methanol (20 mL), five drops of HCl were added to catalyze the reaction. The reaction mixture was kept under stirring for 2 h at room temperature. The resulting solids were filtered off, washed with water and diethyl ether, and dried *in vacuo*.

*2.2.2.1. 3-phenyl-1-pyridin-2-ylprop-2-en-1-one thiosemicarbazone (HPyCTPh) (**1**).* Pale canary yellow solid. Anal. Calcd for $C_{15}H_{14}N_4S$ (%): C, 63.80; H, 5.00; N, 19.84. Found: C, 63.61; H, 4.89; N, 20.10. FW: 282.37 g mol^{-1}. HRMS: *m/z* $[M-H]^-$ calcd for $C_{15}H_{13}N_4S$: 281.0861. Found: 281.0866. UV–vis [DMF, cm^{-1} (log ε)]: 28,011 (4.37). Selected IR bands (KBr, cm^{-1}): (NH_{NH2}) 3416, 3254, (C=N) 1567, (C=S) 750, ρ(py) 538. ^{1}H NMR [200 MHz, DMSO-d$_6$, ppm]: 11.25 (s, 1H, N3–H), 8.64 (d, 1H, H6,

$^3J_{H6\text{-}H5}$ = 4.4 Hz), 8.46 (s, 1H, N4–H), 8.02–7.92 (m, 2H, H3 and N4–H), 7.85 (t, 1H, H4, $^3J_{H4\text{-}H3}$ = $^3J_{H4\text{-}H5}$ = 7.6 Hz), 7.80–7.60 (m, 3H, H10, H12 and H16), 7.51–7.27 (m, 4H, H5, H13, H14 and H15), 7.17 (d, 1H, H9, $^3J_{H9\text{-}H10}$ = 16.1 Hz). ^{13}C NMR [50 MHz, DMSO-d_6, ppm]: 179.0 (C8=S), 155.3 (C2), 148.2 (C6), 145.9 (C7=N), 140.0 (C10), 136.8 (C4), 136.2 (C11), 129.1 (C14), 128.6 (C13 and C15), 127.8 (C12 and C16), 123.8 (C5), 123.6 (C3), 117.1 (C9). Yield: 69%.

*2.2.2.2. 3-(4-chlorophenyl)-1-pyridin-2-ylprop-2-en-1-one thiosemicarbazone (HPy CT4ClPh) (**2**).* Pale canary yellow solid. Anal. Calcd for $C_{15}H_{13}ClN_4S$ (%): C, 56.87; H, 4.14; N, 17.68. Found: C, 56.89; H, 3.99; N, 17.74. FW: 316.81 g mol^{-1}. HRMS: *m/z* $[M-H]^-$ calcd for $C_{15}H_{12}ClN_4S$: 315.0471. Found: 315.0482. UV–vis [DMF, cm^{-1} (log ε)]: 27,548 (4.45). Selected IR bands (KBr, cm^{-1}): (NH_{NH2}) 3422, 3268, (C=N) 1562, (C=S) 778, ρ(py) 548. ^{1}H NMR [200 MHz, DMSO-d_6, ppm]: 11.26 (s, 1H, N3–H), 8.62 (d, 1H, H6, $^3J_{H6\text{-}H5}$ = 4.8 Hz), 8.45 (s, 1H, N4–H), 8.06–7.94 (m, 2H, H3, N4–H), 7.86 (t, 1H, H4, $^3J_{H4\text{-}H3}$ = $^3J_{H4\text{-}H5}$ = 7.4 Hz), 7.82–7.70 (m, 3H, H10, H12 and H16), 7.54–7.38 (m, 3H, H5, H13 and H15), 7.17 (d, 1H, H9, $^3J_{H9\text{-}H10}$ = 16.2 Hz). ^{13}C NMR [50 MHz, DMSO-d_6, ppm]: 179.1 (C8=S), 155.2 (C2), 148.2 (C6), 145.5 (C7=N), 138.5 (C10), 136.8 (C4), 135.2 (C11), 133.5 (C14), 129.4 (C13 and C15), 128.6 (C12 and C16), 123.8 (C5), 123.6 (C3), 117.8 (C9). Yield: 61%.

*2.2.2.3. 3-(4-bromophenyl)-1-pyridin-2-ylprop-2-en-1-one thiosemicarbazone (HPyCT4 BrPh) (**3**).* Yellow solid. Anal. Calcd for $C_{15}H_{13}BrN_4S$ (%): C, 49.87; H, 3.63; N, 15.51. Found: C, 49.75; H, 3.89; N, 15.21. FW: 361.26 g mol^{-1}. HRMS: *m/z* $[M-H]^-$ calcd for $C_{15}H_{12}BrN_4S$: 358.9966. Found: 358.9976. UV–vis [DMF, cm^{-1} (log ε)]: 27,548 (4.45). Selected IR bands (KBr, cm^{-1}): (NH_{NH2}) 3350, 3312, 3236, ($NH_{pyridinium}$) 2690 (broad), (C=N) 1560, (C=S) 780, ρ(py) 554. ^{1}H NMR [200 MHz, DMSO-d_6, ppm]: *E* configuration = 11.44 (s, 1H, N3H), 8.87–8.72 (m, 1H, H6), 8.63 (s, 1H, N4–H), 8.42 (s, 1H, N4–H), 8.34–8.03 (m, 1H, H5), 7.85–7.51 (m, 7H, H5, H3, H12, H16, H13, H15, and H10), 7.13 (d, 1H, H9, $^3J_{H9\text{-}H10}$ = 16.2 Hz); *Z* configuration = 13.07 (s, 1H, SH), 8.87–8.72 (m, 1H, H3), 8.68 (s, 1H, N4–H), 8.34–8.03 (m, 3H, H5, H10, and N4–H), 7.85–7.51 (m, 5H, H4, H12, H16, H13, and H15), 7.37 (m, 1H, H6), 7.13 (d, 1H, H9, $^3J_{H9\text{-}H10}$ = 16.2 Hz). ^{13}C NMR [50 MHz, DMSO-d_6, ppm] main signals: *E* configuration = 179.2 (C8=S), 155.4 (C2), 148.7 (C6), 141.2 (C7=N), 135.7 (C11), 121.4 (C14); *Z* configuration = 178.2 (C8=S), 151.1 (C2), 145.7 (C6), 135.1 (C11), 122.6 (C14). Yield: 75%.

*2.2.2.4. 3-(4-nitrophenyl-1-pyridin-2-ylprop-2-en-1-one thiosemicarbazone (HPyCT4-NO_2Ph) (**4**).* Citrine solid. Anal. Calcd for $C_{15}H_{13}N_5O_2S$ (%): C, 55.03; H, 4.00; N, 21.39. Found: C, 54.83; H, 3.96; N, 21.02. FW: 327.36 g mol^{-1}. HRMS: *m/z* $[M-H]^-$ calcd for $C_{15}H_{12}N_5O_2S$: 326.0712. Found: 326.0718. UV–vis [DMF, cm^{-1} (log ε)]: 32,154 (4.27), 25,316 (4.40). Selected IR bands (KBr, cm^{-1}): (NH_{NH2}) 3418, 3270, (C=N) 1570, (C=S) 822, ρ(py) 596. ^{1}H NMR [200 MHz, DMSO-d_6, ppm]: 11.40 (s, 1H, N3–H), 8.62 (d, 1H, H6, $^3J_{H6\text{-}H5}$ = 4.1 Hz), 8.52 (s, 1H, N4–H), 8.25 (d, 2H, H13 and H15, $^3J_{H13\text{-}H12}$ = $^3J_{H15\text{-}H16}$ = 8.7 Hz), 8.11–7.81 (m, 6H, N4–H, H3, H12, H16, H10, and H4), 7.45 (dd, 1H, H5, $^3J_{H5\text{-}H4}$ = 7.2 Hz, $^3J_{H5\text{-}H3}$ = 4.9 Hz), 7.32 (d, 1H, H9, $^3J_{H9\text{-}H10}$ = 16.1 Hz). ^{13}C NMR [50 MHz, DMSO-d_6, ppm]: 179.2 (C8=S), 155.0 (C2), 148.3 (C6), 147.1 (C7=N), 144.7 (C14), 143.0 (C11), 137.4 (C10), 136.9 (C4), 128.7 (C12 and C16), 123.8 (C3, C5, C13 and C15), 121.1 (C9). Yield: 68%. Upon slow evaporation in 9:1 acetone/DMSO solution, crystals of HPyCT4NO_2Ph were formed.

2.2.3. Synthesis of gallium(III) and zinc(II) complexes with chalcone-derived thiosemicarbazones. Gallium nitrate or zinc chloride (0.5 mmol) was added to a solution of the desired thiosemicarbazone (1 mmol) in methanol (15 mL). The reaction mixture was kept under reflux and stirring for 15 min. Then, a solution containing sodium acetate (1.0 mmol) and the thiosemicarbazone (0.05 mmol) in 5 mL of methanol was added to the reaction mixture which was kept under reflux for 5 h. The obtained solids were filtered off, washed with isopropanol, and dried *in vacuo*.

*2.2.3.1. Bis[3-phenyl-1-pyridin-2-ylprop-2en-1-one thiosemicarbazonato] gallium(III) nitrate [Ga(PyCTPh)$_2$]NO$_3$ (**Ga1**).* Yellow solid. Anal. Calcd for $C_{30}H_{26}GaN_9O_3S_2$ (%): C, 51.89; H, 3.77; N, 18.15. Found: C, 51.95; H, 3.80; N, 18.29. FW: 694.44 g mol^{-1}. HRMS *m/z* $[M - NO_3]^+$ calcd for $C_{30}H_{26}GaN_8S_2$: 631.0978. Found: 631.0971. UV–vis [DMF, cm^{-1} (log ε)]: 32,680 (4.74), 22,779 (4.61), 21,978 (4.62). Selected IR bands (KBr, cm^{-1}): (NH_{NH2}) 3448, 3248, (C=N) 1514, (C=S) 724, ρ(py) 588, (NO_3) 1385, 1324. ^{1}H NMR [200 MHz, DMSO-d$_6$, ppm]: 9.10 (d, 1H, H10, $^3J_{H10\text{-}H9} = 16.2$ Hz), 8.69 (d, 1H, H3, $^3J_{H3\text{-}H4} = 8.3$ Hz), 8.50 (s, 2H, N4–H$_2$), 8.26 (t, 1H, H4, $^3J_{H4\text{-}H3} = {}^3J_{H4\text{-}H5} = 7.8$ Hz), 8.04–7.87 (m, 3H, H6, H12, and H16), 7.76 (d, 1H, H9, $^3J_{H9\text{-}H10} = 16.2$ Hz), 7.63 (t, 1H, H5, $^3J_{H5\text{-}H4} = 5.2$ Hz, $^3J_{H5\text{-}H3} = 7.5$ Hz), 7.57–7.39 (m, 3H, H13, H14, and H15). ^{13}C NMR [50 MHz, DMSO-d$_6$, ppm]: 178.3 (C8=S), 145.9 (C2), 145.1 (C6), 144.6 (C10), 142.8 (C4), 139.0 (C7=N), 137.0 (C11), 130.4 (C14), 129.3 (C13 and C15), 128.6 (C12 and C16), 127.1 (C5), 124.0 (C3), 115.7 (C9). Molar conductivity (1 mmol L^{-1}, DMF): 69.5 Ω^{-1} cm^2 mol^{-1}. Yield: 70%.

*2.2.3.2. Bis[3-(4-chlorophenyl)-1-pyridin-2-ylprop-2en-1-one thiosemicarbazonato] gallium (III) nitrate [Ga(PyCT4ClPh)$_2$]NO$_3$ (**Ga2**).* Yellow solid. Anal. Calcd for $C_{30}H_{24}Cl_2GaN_9O_3S_2$ (%): C, 47.20; H, 3.17; N, 16.51. Found: C, 47.07; H, 3.19; N, 16.65. FW: 763.33 g mol^{-1}. HRMS: *m/z* $[M - NO_3]^+$ calcd for $C_{30}H_{24}Cl_2GaN_8S_2$: 699.0198. Found: 699.0208. UV–vis [DMF, cm^{-1} (log ε)]: 32,051 (4.84), 22,728 (4.71), 21,930 (4.73). Selected IR bands (KBr, cm^{-1}): (NH_{NH2}) 3454, 3278, (C=N) 1520, (C=S) 728, ρ(py) 649, (NO_3) 1384, 1285. ^{1}H NMR [200 MHz, DMSO-d$_6$, ppm]: 9.16 (d, 1H, H10, $^3J_{H10\text{-}H9} = 15.9$ Hz), 8.69 (d, 1H, H3, $^3J_{H3\text{-}H4} = 8.1$ Hz), 8.54 (s, 2H, N4–H$_2$), 8.24 (t, 1H, H4, $^3J_{H4\text{-}H3} = {}^3J_{H4\text{-}H5} = 7.7$ Hz), 8.00 (d, 2H, H12 and H16, $^3J_{H13\text{-}H12} = {}^3J_{H15\text{-}H16} = 8.3$ Hz), 7.92 (d, 1H, H6, $^3J_{H6\text{-}H5} = 4.6$ Hz), 7.74 (d, 1H, H9, $^3J_{H9\text{-}H10} = 15.9$ Hz), 7.68–7.51 (m, 3H, H5, H13, and H15). ^{13}C NMR [50 MHz, DMSO-d$_6$, ppm]: 178.6 (C8=S), 146.0 (C2), 144.6 (C6), 143.8 (C10), 142.8 (C4), 138.5 (C7=N), 136.0 (C11), 134.8 (C14), 130.3 (C13 and C15), 129.3 (C12 and C16), 127.0 (C5), 123.9 (C3), 116.2 (C9). Molar conductivity (1 mmol L^{-1}, DMF): 75.8 Ω^{-1} cm^2 mol^{-1}. Yield: 65%.

*2.2.3.3. Bis[3-(4-bromophenyl)-1-pyridin-2-ylprop-2en-1-one thiosemicarbazonato] gallium (III) nitrate [Ga(PyCT4BrPh)$_2$]NO$_3$ (**Ga3**).* Yellow solid. Anal. Calcd for $C_{30}H_{24}Br_2GaN_9O_3S_2$ (%): C, 42.28; H, 2.84; N, 14.79. Found: C, 42.38; H, 2.95; N, 14.75. FW: 870.24 g mol^{-1}. HRMS: *m/z* $[M - NO_3]^+$ calcd for $C_{30}H_{24}Br_2GaN_8S_2$: 786.9188. Found: 786.9213. UV–vis [DMF, cm^{-1} (log ε)]: 31,949 (4.81), 22,831 (4.65), 21,930 (4.68). Selected IR bands (KBr, cm^{-1}): (NH_{NH2}) 3456, 3277, (C=N) 1519, (C=S) 728, ρ(py) 651, (NO_3) 1385, 1299. ^{1}H NMR [200 MHz, DMSO-d$_6$, ppm]: 9.18 (d, 1H, H10, $^3J_{H10\text{-}H9} = 15.9$ Hz), 8.71 (d, 1H, H3, $^3J_{H3\text{-}H4} = 8.3$ Hz), 8.54 (s, 2H, N4–H$_2$), 8.25 (t, 1H, H4, $^3J_{H4\text{-}H3} = {}^3J_{H4\text{-}H5} = 7.8$ Hz), 8.02–7.86 (m, 3H, H6, H12, and H16), 7.84–7.67 (m, 3H, H9, H13, and H15), 7.61 (d, 1H, H5, $^3J_{H5\text{-}H4} = {}^3J_{H5\text{-}H6} = 7.0$ Hz). ^{13}C NMR [50 MHz,

DMSO-d_6, ppm]: 178.6 (C8=S), 145.9 (C2), 144.6 (C6), 143.9 (C10), 142.8 (C4), 138.4 (C7=N), 136.4 (C11), 132.2 (C13 and C15), 130.5 (C12 and C16), 127.0 (C5), 123.6 (C14), 123.8 (C3), 116.2 (C9). Molar conductivity (1 mmol L^{-1}, DMF): 67.9 Ω^{-1} cm^2 mol^{-1}. Yield: 72%.

*2.2.3.4. Bis[3-(4-nitrophenyl)-1-pyridin-2-ylpro-2-en-1-one thiosemicarbazonato] gallium (III) nitrate [Ga(PyCT4NO$_2$Ph)$_2$]NO$_3$ (**Ga4**).* Orange solid. Anal. Calcd for $C_{30}H_{24}GaN_{11}O_7S_2$ (%): C, 45.93; H, 3.08; N, 19.64. Found: C, 45.85; H, 3.03; N, 19.62. FW: 784.44 g mol^{-1}. HRMS: *m/z* $[M - NO_3]^+$ calcd for $C_{30}H_{24}GaN_{10}O_4S_2$: 721.0679. Found: 721.0667. UV–vis [DMF, cm^{-1} (log ε)]: 29,851 (4.79), 21,787 (4.68), 21,231 (4.70). Selected IR bands (KBr, cm^{-1}): (NH_{NH2}) 3446, 3296, (C=N) 1514, (C=S) 728, ρ(py) 658, (NO_3) 1385, 1295. ^{1}H NMR [200 MHz, DMSO-d_6, ppm]: 9.28 (d, 1H, H10, $^3J_{H10\text{-}H9}$ = 15.9 Hz), 8.88 (s, 2H, N4–H_2), 8.73 (d, 1H, H3, $^3J_{H3\text{-}H4}$ = 8.1 Hz), 8.47–8.16 (m, 5H, H13, H15, H4, H12, and H16), 8.03–7.83 (m, 2H, H6, and H9), 7.63 (dd, 1H, H5, $^3J_{H5\text{-}H4}$ = 7.1 Hz, $^3J_{H5\text{-}H6}$ = 5.3 Hz). ^{13}C NMR [50 MHz, DMSO-d_6, ppm]: 178.8 (C8=S), 147.2 (C2), 145.4 (C14), 144.3 (C6), 143.4 (C11), 142.5 (C4), 141.8 (C10), 137.3 (C7=N), 129.0 (C12 and C16), 126.6 (C5), 124.0 (C13 and C15), 123.4 (C3), 119.1 (C9). Molar conductivity (1 mmol L^{-1}, DMF): 66.3 Ω^{-1} cm^2 mol^{-1}. Yield: 84%.

*2.2.3.5. Bis[3-phenyl-1-pyridin-2-ylprop-2-en-1-one thiosemicarbazonato] zinc(II) [Zn(PyCTPh)$_2$] (**Zn1**).* Yellow solid. Anal. Calcd for $C_{30}H_{26}N_8S_2Zn$ (%): C, 57.37; H, 4.17; N, 17.84. Found: C, 57.30; H, 4.13; N, 17.79. FW: 628.10 g mol^{-1}. UV–vis [DMF, cm^{-1} (log ε)]: 22,676 (4.60). Selected IR bands (KBr, cm^{-1}): (NH_{NH2}) 3442, 3304, (C=N) 1510, (C=S) 726, ρ(py) 582. ^{1}H NMR [200 MHz, DMSO-d_6, δ (ppm)]: 8.23 (d, 1H, H10, $^3J_{H10\text{-}H9}$ = 16.7 Hz), 8.04 (d, 1H, H3, $^3J_{H3\text{-}H4}$ = 8.6 Hz), 7.94–7.81 (m, 2H, H4, and H6), 7.77 (d, 2H, H12 and H16, $^3J_{H12\text{-}H13}$ = $^3J_{H16\text{-}H15}$ = 7.3 Hz), 7.66 (d, 1H, H9, $^3J_{H9\text{-}H10}$ = 16.7 Hz), 7.51–7.23 (m, 6H, H14, N4–H_2, H13, H15, and H5). ^{13}C NMR [50 MHz, DMSO-d_6, ppm]: 183.3 (C8=S), 149.7 (C2), 146.4 (C6), 139.5 (C7=N), 138.9 (C4), 137.8 (C10), 137.3 (C11), 128.7 (C13 and C15), 128.5 (C14), 127.2 (C12 and C16), 123.5 (C5), 121.7 (C3), 118.5 (C9). Molar conductivity (1 mmol L^{-1}, DMF): 0.5 Ω^{-1} cm^2 mol^{-1}. Yield: 92%.

*2.2.3.6. Bis[3-(4-chlorophenyl)-1-pyridin-2-ylprop-2en-1-one thiosemicarbazonato] zinc(II) [Zn(PyCT4ClPh)$_2$] (**Zn2**).* Yellow solid. Anal. Calcd for $C_{30}H_{24}Cl_2N_8S_2Zn$ (%): C, 51.70; H, 3.47; N, 16.08. Found: C, 51.76; H, 3.50; N, 16.12. FW: 696.99 g mol^{-1}. UV–vis [DMF, cm^{-1} (log ε)]: 22,371 (4.64). Selected IR bands (KBr, cm^{-1}): (NH_{NH2}) 3448, 3288, (C=N) 1512, (C=S) 730, ρ(py) 636. ^{1}H NMR [200 MHz, DMSO-d_6, ppm]: 8.42 (d, 1H, H10, $^3J_{H10\text{-}H9}$ = 16.4 Hz), 8.08 (d, 1H, H3, $^3J_{H3\text{-}H4}$ = 8.1 Hz), 7.92–7.75 (m, 4H, H4, H6, H12, and H16), 7.73 (d, 1H, H9, $^3J_{H9\text{-}H10}$ = 16.6 Hz), 7.55–7.37 (m, 4H, N4–H_2, H13, and H15), 7.28 (t, 1H, H5, $^3J_{H5\text{-}H6}$ = $^3J_{H5\text{-}H4}$ = 7.0 Hz). ^{13}C NMR [50 MHz, DMSO-d_6, ppm]: 183.6 (C8=S), 149.8 (C2), 146.3 (C6), 138.9 (C4), 138.6 (C7=N), 136.8 (C10), 136.4 (C11), 132.8 (C14), 128.8 (C13 and C15), 128.6 (C12 and C16), 123.4 (C5), 121.4 (C3), 118.8 (C9). Molar conductivity (1 mmol L^{-1}, DMF): 0.2 Ω^{-1} cm^2 mol^{-1}. Yield: 96%.

*2.2.3.7. Bis[3-(4-bromophenyl)-1-pyridin-2-ylprop-2en-1-one thiosemicarbazonato] zinc(II) [Zn(PyCT4BrPh)$_2$] (**Zn3**).* Yellow solid. Anal. Calcd for $C_{30}H_{24}Br_2N_8S_2Zn$ (%): C, 45.85; H, 3.08; N, 14.26. Found: C, 45.79; H, 3.11; N, 14.34. FW: 785.90 g mol^{-1}. UV–vis [DMF, cm^{-1} (log ε)]: 22,321 (4.61). Selected IR bands (KBr, cm^{-1}): (NH_{NH2}) 3436, 3290, (C=N) 1516, (C=S) 728, ρ(py) 635. ^{1}H NMR [200 MHz, DMSO-d_6, ppm]: 8.41 (d,

1H, H10, $^{3}J_{H10\text{-}H9} = 16.3$ Hz), 8.07 (d, 1H, H3, $^{3}J_{H3\text{-}H4} = 8.0$ Hz), 7.94–7.55 (m, 7H, H4, H6, H12, H16, H3, H13, and H15), 7.46 (s, 2H, N4–H_2), 7.27 (t, 1H, H5, $^{3}J_{H5\text{-}H4} = {}^{3}J_{H5\text{-}H6} = 6.4$ Hz). ^{13}C NMR [50 MHz, DMSO-d_6, ppm]: 183.7 (C8=S), 149.8 (C2), 146.3 (C6), 138.9 (C4), 138.6 (C7=N), 136.9 (C10), 136.8 (C11), 131.5 (C13 and C15), 129.1 (C12 and C16), 123.4 (C5), 121.4 (C3 and C14), 118.8 (C9). Molar conductivity (1 mmol L^{-1}, DMF): 2.7 Ω^{-1} cm^2 mol^{-1}. Yield: 73%.

*2.2.3.8. Bis[3-(4-nitrophenyl)-1-pyridin-2-ylprop-2en-1-one thiosemicarbazonato] zinc(II) [Zn(PyCT4NO$_2$Ph)$_2$] (**Zn4**).* Orange-red solid. Anal. Calcd for $C_{30}H_{24}N_{10}O_4S_2Zn$ (%): C, 50.18; H, 3.37; N, 19.51. Found: C, 50.05; H, 3.34; N, 19.46. FW: 718.06 g mol^{-1}. UV–vis [DMF, cm^{-1} (log ε)]: 31,348 (4.67), 26,385 (4.46), 20,877 (4.61). Selected IR bands (KBr, cm^{-1}): (NH_{NH2}) 3446, 3296, (C=N) 1512, (C=S) 727, ρ(py) 630. ^{1}H NMR [200 MHz, DMSO-d_6, ppm]: 8.73 (d, 1H, H10, $^{3}J_{H10\text{-}H9} = 16.2$ Hz), 8.28 (d, 1H, H3, $^{3}J_{H3\text{-}H4} = 8.7$ Hz), 8.20–7.99 (m, 3H, H3, H13, and H15), 7.97–7.61 (m, 6H, H6, H12, H16, H9, and N4–H_2), 7.29 (dd, 1H, H5, $^{3}J_{H5\text{-}H4} = 7.2$ Hz, $^{3}J_{H5\text{-}H6} = 5.3$ Hz). ^{13}C NMR [50 MHz, DMSO-d_6, ppm]: 184.5 (C8=S), 149.8 (C2), 146.6 (C14), 146.3 (C6), 144.7 (C11), 139.1 (C4), 137.4 (C7=N), 135.9 (C10), 128.0 (C12 and C16), 123.8 (C13 and C15), 123.4 (C5), 121.7 (C3), 121.2 (C9). Molar conductivity (1 mmol L^{-1}, DMF): 0.5 Ω^{-1} cm^2 mol^{-1}. Yield: 95%.

2.3. *Crystal structure determination*

The crystal structure of **4** was determined using single-crystal X-ray diffractometry. Molecular plot and crystal packing figures were prepared using ORTEP [20] and MERCURY [21], respectively. Tables were generated using WINGX suite [22]. A summary of the crystal data, data collection details, and refinement results are listed in table 1.

2.4. *In vitro antimicrobial activity*

Antibacterial activity was evaluated by minimum inhibitory concentration (MIC) using the macrodilution test [23,24]. *Staphylococcus aureus* ATCC 6538 or *P. aeruginosa* ATCC 27853 stored in Mueller Hinton broth were subcultured for testing in the same medium and grown at 37 °C. Then, the bacterial cells were suspended, according to the McFarland protocol [24] in saline solution, to produce a suspension of 10^5 colony-forming units/mL (CFU mL^{-1}). Serial dilutions of the compounds, previously dissolved in DMSO, were prepared in test tubes to final concentrations of 512, 256, 128, 64, 32, 16, 8, 4, 2 and 1 μg mL^{-1}. A 24-h-old inoculum (100 μL) was added to each tube. The MIC, defined as the lowest concentration of the test compound which inhibits the visible growth after 20 h, was determined visually after incubation for 20 h at 37 °C. Tests using tetracycline as reference and DMSO as negative control were carried out in parallel. All tests were performed in triplicate with full agreement between the results.

Antifungal activity was evaluated by MIC using the macrodilution test [23,25]. *Candida albicans* ATCC 10231 stored in Sabouraud broth was subcultured for testing in the same medium and grown at 37 °C. Then, yeast cells were suspended according to the McFarland protocol [25] in saline solution to produce a suspension of 10^5 CFU mL^{-1}. Serial dilutions of the compounds, previously dissolved in DMSO, were prepared in test tubes to final concentrations of 512, 256, 128, 64, 32, 16, 8, 4, 2, and 1 μg mL^{-1}. A 24-h-old inoculum

Table 1. Crystal data and structure refinement results for **4**.

Compound	HPyCT4NO$_2$Ph (**4**)
Empirical formula	$C_{15}H_{13}N_5O_2S$
Molecular weight (g mol^{-1})	327.36
Crystal system, space group	Monoclinic, *Pc*
Unit cell dimensions	
a (Å)	7.8859(1)
b (Å)	16.7965(2)
c (Å)	11.2801(2)
α (°)	90
β (°)	93.427(1)
γ (°)	90
V (Å^3)	1491.44(4)
Z	4
D_{calc} (g cm^{-3})	1.458
F(0 0 0)	680
Crystal size (mm)	0.54 × 0.24 × 0.10
Absorption coefficient (mm^{-1})	0.235
θ range for data collection (°)	2.86 to 26.37
Index ranges	$-9 \leqslant h \leqslant 9$ $-20 \leqslant k \leqslant 20$ $-14 \leqslant l \leqslant 14$
Reflections collected	48,255
Reflections unique/*R*(int)	3054/0.0394
Completeness to theta = 26.37° (%)	99.9
Max. and min. transmission	0.9769 and 0.8837
Final *R* indices [I > 2σ(I)]	*R*1 = 0.0241, *wR*2 = 0.0670
R indices (all data)	*R*1 = 0.0254, *wR*2 = 0.0675
Goodness-of-fit on F^2	1.066
Absolute structure parameter	0.10(5)
Largest diff. peak and hole (e Å^{-3})	0.222/−0.171

(100 µL) was added to each tube. The MIC was determined visually after incubation for 20 h at 37 °C. Tests using fluconazole as reference and DMSO as negative control were carried out in parallel. No inhibition was observed with 5% v/v DMSO. All tests were performed in triplicate with full agreement between the results.

3. Results and discussion

3.1. *Formation of chalcone-derived thiosemicarbazones and their metal complexes*

Formation of the thiosemicarbazones (**1–4**) was confirmed by microanalyses, infrared, NMR, and HRMS data. Microanalyses and molar conductivities were compatible with the formation of the gallium(III) complexes [Ga(PyCTPh)$_2$]NO$_3$ (**Ga1**), [Ga(PyCT4ClPh)$_2$]NO$_3$ (**Ga2**), [Ga(PyCT4BrPh)$_2$]NO$_3$ (**Ga3**), and [Ga(PyCT4NO$_2$Ph)$_2$]NO$_3$ (**Ga4**) and the zinc(II) complexes [Zn(PyCTPh)$_2$] (**Zn1**), [Zn(PyCT4ClPh)$_2$] (**Zn2**), [Zn(PyCT4BrPh)$_2$] (**Zn3**), and [Zn(PyCT4NO$_2$Ph)$_2$] (**Zn4**). In all complexes, the thiosemicarbazone is attached to the metal center as an anion.

3.1.1. HRMS data. HRMS data were used to further characterize the thiosemicarbazones and their complexes. The thiosemicarbazones exhibited a peak at *m/z* 281.0866 (**1**),

315.0482 (**2**), 358.9976 (**3**), and 326.0718 (**4**) in the negative ionization mode which was attributed to the ion fragment $[M-H]^-$, indicating the presence of an anionic thiosemicarbazone. The appearance of this ion is associated with the high stability of the anionic form resulting from increased conjugation.

In spectra of the gallium(III) complexes, a peak at *m/z* 631.0971 (**Ga1**), 699.0208 (**Ga2**), 786.9213 (**Ga3**), and 721.0667 (**Ga4**) was observed in the positive ionization mode, due to formation of $[Ga(L)_2]^+$. The presence of this peak is in accordance with molar conductivity data that indicated that the complexes are 1 : 1 electrolytes in solution.

For the zinc(II) complexes, no peaks attributable to ionization were observed, in accordance with molar conductivity data which indicated that the complexes are nonelectrolytes.

3.1.2. Electronic spectra. The electronic spectra of the chalcone precursors showed an absorption at *ca*. 30,769–31,546 cm^{-1}, attributable to the $n\rightarrow\pi^*$ transition of the enone function. Upon formation of the thiosemicarbazones, absorptions at 25,316–28,011 cm^{-1}, attributable to $n\rightarrow\pi^*$ transitions of the azomethine and thioamide functions overlapped in the same envelope, were observed [26]. In the case of **4**, the transitions appeared at lower energies and a $\pi\rightarrow\pi^*$ transition was also noticed at 32,154 cm^{-1}, which could not be observed in spectra of **1–3**. This difference is probably due to the presence of the electron-withdrawing NO_2 group in **4**.

In spectra of the gallium(III) complexes, the $\pi\rightarrow\pi^*$ transitions of the aromatic rings are at *ca*. 29,851–32,680 cm^{-1}. Two $n\rightarrow\pi^*$ transitions attributed to C=N and C=S were observed at *ca*. 21,787–22,831 cm^{-1} and *ca*. 21,231–21,978 cm^{-1}, respectively. In the zinc(II) complexes, the C=N and C=S $n\rightarrow\pi^*$ transitions were observed at *ca*. 20,877–22,371 cm^{-1}.

Upon coordination to both metals, the $n\rightarrow\pi^*$ transitions of the azomethine and thioamide functions shifted to lower energies due to the formation of a highly delocalized system upon deprotonation of the ligand [27,28].

3.1.3. Infrared spectra. Upon formation of the thiosemicarbazones, the ν(C=O) vibration at 1670–1677 cm^{-1} in infrared spectra of the chalcones disappeared along with the appearance of a new absorption at 1560–1570 cm^{-1}, attributed to ν(C=N) [29]. New absorptions were observed at 3150–3450 cm^{-1}, which were attributed to ν(N–H) of the thioamide [5,29], and a strong absorption at 750–822 cm^{-1} that was assigned to ν(C=S) [29]. In the spectrum of **3,** a new absorption was observed at 2500–2800 cm^{-1} which was attributed to ν(S–H), indicating the presence of thione-thiol tautomerism [30], or to ν(N–H) of a pyridinium ion [31].

The ν(C=N) absorption underwent a shift in spectra of the complexes, suggesting coordination of the imine nitrogen [5,6,32]. The ν(C=S) vibration at 750–822 cm^{-1} in the uncomplexed thiosemicarbazones shifted to 724–730 cm^{-1} in spectra of the complexes, indicating coordination of sulfur [5,6,16]. The in-plane deformation mode of the pyridinering at 538–596 cm^{-1} in spectra of the free bases shifted to 588–658 cm^{-1} in the complexes, suggesting coordination of the heteroaromatic nitrogen [16,29].

For the gallium(III) complexes, new absorptions attributed to the symmetric and asymmetric stretching of NO from nitrate were observed at *ca*. 1385 cm^{-1} and 1285–1324 cm^{-1}, respectively [6,16,33].

3.1.4. NMR spectra. Immediately after dissolution, only one signal was observed for each hydrogen atom in spectra of **1**, **2,** and **4**, but duplicate signals were found for carbon atoms due to the time required for recording ^{13}C NMR spectra. The signal of N3–H was observed at 11.21, 11.26, and 11.40 ppm for **1**, **2,** and **4**, respectively. ^{1}H NMR spectra registered one hour after dissolution showed duplicated signals, in accordance with the presence of two species in solution. The signals of all hydrogen and carbon atoms are duplicated in ^{1}H and ^{13}C NMR spectra of **3**, even immediately after dissolution, indicating the presence of two isomers in DMSO-d_6.

An NOEDIFF experiment was recorded for **1** immediately after dissolution by irradiating at 11.21 ppm (figure 3), which is the position of N3–H. One NOE signal at 7.76 ppm ($J = 16$ Hz), attributed to H10, indicates that the compound adopts the *E* configuration in relation to the C7-N2 bond. Hence, the predominant form of **1** is *E*. Similarly, the *E* configuration is dominant for **2** and **4**. ^{1}H NMR spectra of **1**, **2,** and **4** registered one hour after dissolution showed a signal at 12.89, 13.07, and 13.33 ppm, respectively, which is characteristic of the *Z* isomer, in which N3–H is hydrogen bonded to the pyridine nitrogen. The presence of the *E* and *Z* isomers is frequently observed for 2-benzoylpyridine-derived thiosemicarbazones [31,34,35].

Hereafter, attributions are given only for the main isomer (*E*) of **1**, **2,** and **4**. The high value of the H9/H10 coupling constant ($J = 16$ Hz) indicates that these two hydrogen atoms are *trans* to each other in relation to the C9–C10 bond and that the configuration is *E* in relation to this bond. Thus, immediately after dissolution, the compounds adopt the *EE* configuration in relation to C7–N2 and C9–C10. After one hour, one observes the presence of the *EE* and *ZE* configurations in equilibrium in the solution. Crystal structure determination of **4** revealed that the compound adopts the *ZE* configuration.

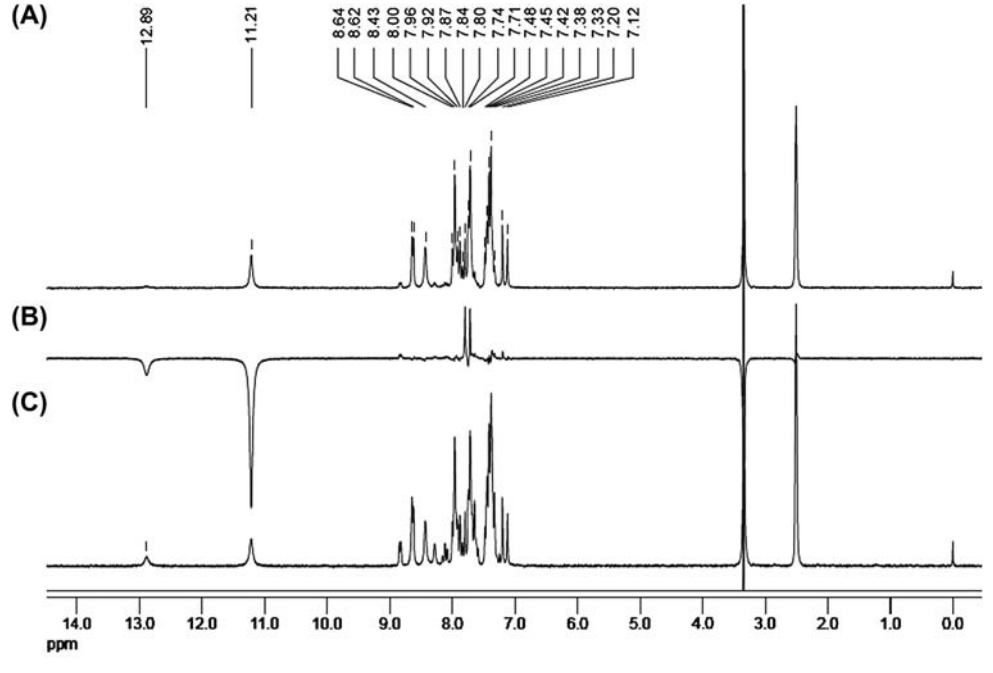

Figure 3. ^{1}H NMR spectra of HPyCTPh (**1**) (DMSO-d_6, 200 MHz). (a) Spectrum obtained immediately after dissolution. (b) NOEDIFF spectrum (irradiation at 11.21 ppm). (c) Spectrum obtained 1 h after dissolution.

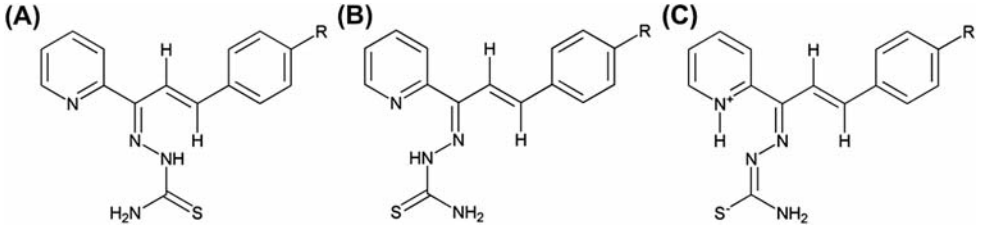

Figure 4. Generic structure of chalcone-derived thiosemicarbazones showing the *E* (A) and *Z* (B) configurational isomers, and the *Z* zwitterionic form (C).

NMR data do not allow the attribution of the conformation in relation to the C8–N3 bond. The two resonances observed for $N4H_2$ in the ^{1}H NMR spectra of **1**, **2,** and **4** indicated hindered rotation around the –C=S–NH_2 bond due to its partial double bond character [36].

Signals at 13.07 and 11.44 ppm in the spectrum of **3** may be attributed to N3–H of the *Z* and *E* isomers, respectively. The absence of the signal at 4.0 ppm attributable to S–H proton in the spectrum of **3** provided strong evidence for the presence of the thione form in solution [37]. Since the *Z* isomer is present, transference of the hydrogen from N3–H to the pyridine nitrogen could have occurred. Therefore, the broad absorption at 2500–2800 cm^{-1} in the infrared spectrum of **3** is most likely attributable to ν(N–H) of the pyridinium ion, with formation of a zwitterion containing a sulfur in the thiolate form in a highly delocalized system involving the heteroaromatic ring and the thiosemicarbazone chain (figure 4).

Only one signal was observed for each hydrogen atom and each carbon atom in the NMR spectra of the complexes. In the ^{1}H NMR spectra of all complexes, the signal of N3–H was no longer observed, indicating deprotonation upon complexation and the presence of an anionic thiosemicarbazones. Only one signal was observed for $N4H_2$ in accord with the higher rigidity of the C8–N3 bond in the complexes, which acquired double bond character upon deprotonation at N3.

In ^{13}C NMR spectra of the complexes, the signals of C7 and C8 shifted in relation to their positions in the free thiosemicarbazone, suggesting coordination through the sulfur and the imine nitrogen. The ^{1}H and ^{13}C signals of the pyridine hydrogen and carbon atoms underwent significant shifts in the spectra of the complexes, suggesting coordination through the aromatic nitrogen. Hence, in all complexes, two thiosemicarbazone ligands are attached to the metal through the Npy–N–S chelating system and adopt the *EZE* conformation in relation to the C7–N2, N3–C8, and C9–C10 bonds.

3.2. *Crystal structure of HPyCT4NO$_2$Ph (4)*

The ORTEP diagram of **4** is shown in figure 5. Selected intramolecular bond lengths and angles and hydrogen bonding parameters in the structure are given in tables 2 and 3, respectively. Figure 6 shows a perspective view of the crystal packing.

4 crystallized in the monoclinic system, space group *Pc*, with two independent molecules (**A** and **B**) in the asymmetric unit (figure 5). In **A,** sulfur was numbered S1 and in molecule **B,** S11. In these molecules, the C=N–N–C(=S)N skeleton is almost planar (*rms* deviation from the least-squares plane of 0.0735 and 0.0177 Å for **A** and **B**,

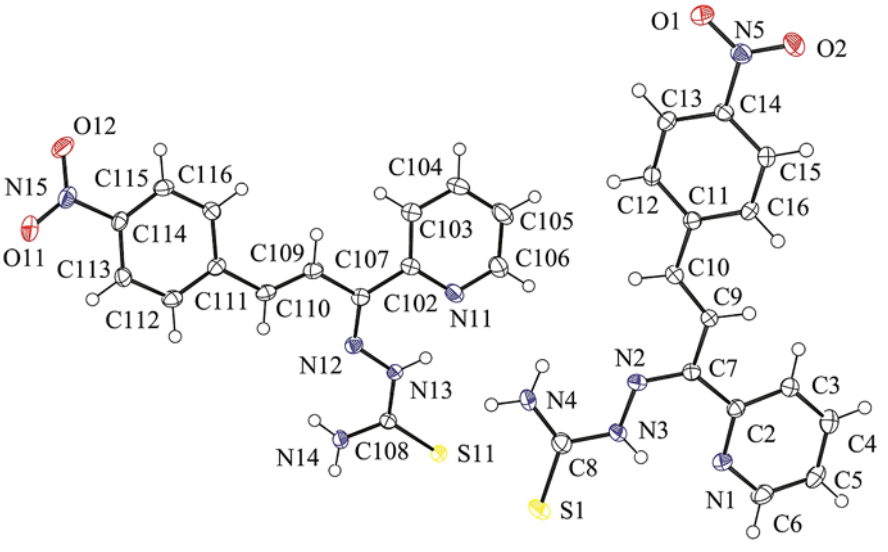

Figure 5. ORTEP diagram for HPyCT4NO$_2$Ph (**4**) with thermal ellipsoids at the 50% probability level and labeling scheme of the nonhydrogen atoms. Hydrogen atoms are drawn as circles of arbitrary radii.

respectively). The angles between the plane of the thiosemicarbazone moiety and the plane of the pyridine ring are quite similar in the two molecules, i.e. 14.87(8)° and 13.36(9)° in **A** and **B**, respectively. However, the angle between the plane of the chalcone-derived chain

Table 2. Selected bond lengths (Å) and angles (°) for **4**.

Bond lengths			
S1–C8	1.681(2)	S11–C108	1.675(2)
N3–C8	1.363(3)	N13–C108	1.360(3)
N3–N2	1.361(2)	N13–N12	1.354(2)
N2–C7	1.309(3)	N12–C107	1.300(3)
N1–C2	1.347(3)	N11–C102	1.348(3)
C7–C2	1.483(3)	C107–C102	1.498(3)
C7–C9	1.473(3)	C107–C109	1.471(3)
C10–C9	1.335(3)	C110–C109	1.328(3)
C11–C10	1.462(3)	C111–C110	1.466(3)
C11–C12	1.397(3)	C111–C112	1.390(3)
C11–C16	1.408(3)	C111–C116	1.407(3)
Angles			
N1–C2–C7	117.9(2)	N11–C102–C107	117.4(2)
C9–C7–C2	118.0(2)	C109–C107–C102	118.1(2)
N2–C7–C9	114.8(2)	N12–C107–C109	115.4(2)
C7–N2–N3	119.4(2)	C107–N12–N13	119.4(2)
N2–N3–C8	118.6(2)	N12–N13–C108	120.2(2)
N3–C8–S1	118.8(2)	N13–C108–S11	119.1(2)
N4–C8–N3	116.8(2)	N14–C108–N13	117.3(2)
C10–C9–C7	125.5(2)	C110–C109–C107	124.6(2)
C9–C10–C11	124.9(2)	C109–C110–C111	126.0(2)
C12–C11–C10	119.0(2)	C112–C111–C110	118.2(2)
C13–C12–C11	121.5(2)	C113–C112–C111	121.3(2)
C16–C11–C10	122.8(2)	C116–C111–C110	123.0(2)
C12–C11–C16	118.3(2)	C112–C111–C116	118.9(2)

Table 3. Hydrogen bonds for **4** [Å and °].

D–H–A	D–H	H–A	D–A	D–H–A
N3–H3–N1	0.88	1.95	2.632(3)	132.9
N4–H4B–S11[a]	0.88	2.74	3.556(2)	155.5
N13–H13–N11	0.88	1.90	2.598(3)	135.1
N14–H14A–O2[b]	0.88	2.44	3.160(2)	139.1
N14–H14B–O12[c]	0.88	2.36	3.225(3)	165.7

Notes: Symmetry transformations used to generate equivalent atoms: [a] $=x-1, y, z$; [b] $=x+1, y-1, z$; [c] $=x+1, y, z+1$.

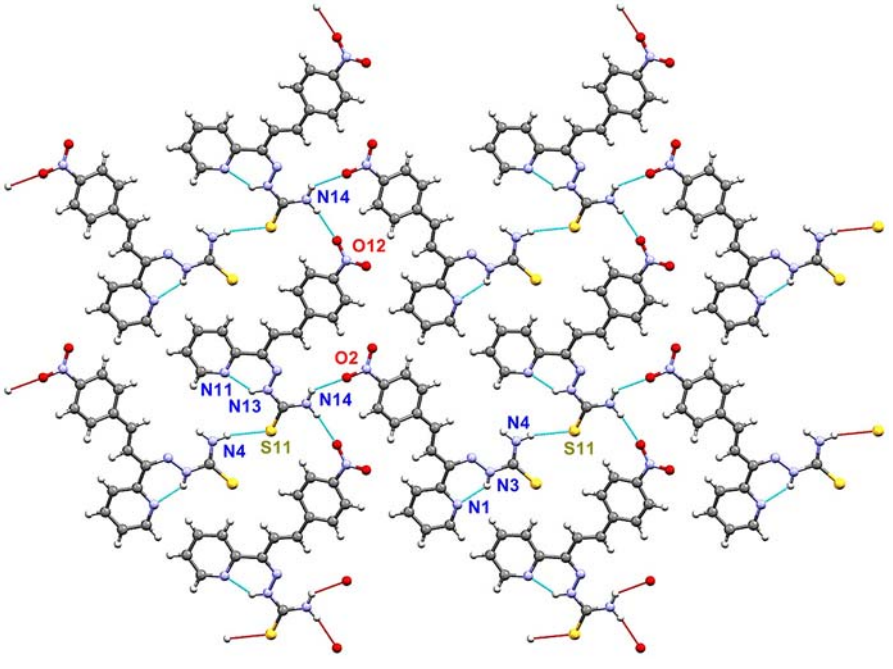

Figure 6. View of the crystal packing of HPyCT4NO$_2$Ph (**4**).

attached to C7 and the plane of the pyridine ring is different for the two molecules, i.e. 32.87(6)° and 9.00(9)°, for **A** and **B**, respectively.

The molecule of **4** adopts the *ZEE* conformation in relation to the C7–N2, N3–C8, and C9–C10 bonds. The presence of the *ZE* conformation in relation to C7–N2 and N3–C8 is quite common in 2-benzoylpyridine-derived thiosemicarbazones [29,34,38]. In fact, bond lengths within the pyridine ring and the thiosemicarbazone chain in **4** (table 2) are very similar to those of 2-benzoylpyridine thiosemicarbazone (H2BPyTSC) [38]. Intramolecular N3–H3···N1 and N13–H13···N11 hydrogen bonds were observed in molecules **A** and **B**, respectively, which result in the *Z* configuration in relation to the C7–N2 bond.

In the molecular packing of **4,** intermolecular hydrogen bonds involving N4–H or N14–H and S11, O2, and O12 lead to formation of an infinite 2D network parallel to the (1 0 −1) plane (see table 3 and figure 6).

3.3. *In vitro antimicrobial activity*

Table 4 reports the MIC of the studied compounds against *S. aureus*, *P. aeruginosa,* and *C. albicans*, together with MIC values for the reference drugs tetracycline hydrochloride and fluconazole.

The chalcones, thiosemicarbazones (**1–4**), and zinc(II) complexes (**Zn1**–**Zn4**) are not active against *P. aeruginosa* in the assayed conditions. The activity of the chalcones followed the order PyCPh < PyC4ClPh < PyC4BrPh ~ PyC4NO_2Ph against *S. aureus* and the order PyCPh < PyC4ClPh ~ PyC4BrPh < PyC4NO_2Ph against *C. albicans*, indicating that the presence of the halogen or the nitro substituent in the *para* position of the chalcone phenyl ring leads to activity improvement. The chalcone-derived thiosemicarbazones, except **4**, were in general more active than the parent compounds against *S. aureus* and *C. albicans*. The activities of the thiosemicarbazones followed the order **1** < **2** < **3** against *S. aureus* and the order **3** < **1** < **2** against *C. albicans*. Interestingly, the nitro derivative (**4**) proved to be inactive against both micro-organisms in the assayed conditions. The low solubility of **4** may, at least in part, account for its lack of activity.

Coordination to zinc(II) resulted in activity improvement of the thiosemicarbazones against *S. aureus,* but was not a good strategy for activity enhancement against *C. albicans*. Although gallium nitrate proved to be inactive against the assayed micro-organisms, coordination of gallium(III) to the thiosemicarbazones significantly enhanced antimicrobial activity. Coordination to gallium(III) resulted in activity improvement of all thiosemicarbazones against the three studied micro-organism strains, indicating this to be an effective strategy for antimicrobial activity enhancement. As previously suggested, the mechanism of antibacterial [6] and antifungal [13] activity of gallium(III) complexes probably involves perturbation of iron metabolism.

Table 4. MIC against *S. aureus* ATCC 6538, *P. aeruginosa* ATCC 27853, and *C. albicans* ATCC 10231 for the chalcones, thiosemicarbazones, their metal complexes, the metal salts, tetracycline, and fluconazole.

	MIC ($\mu mol\,L^{-1}$)		
Compounds	*S. aureus*	*P. aeruginosa*	*C. albicans*
PyCPh	30.3	>145	31.1
HPyCTPh (**1**)	21.3	>84.1	11.3
[Ga(PyCTPh)$_2$]NO_3 (**Ga1**)	4.46	17.83	16.8
[Zn(PyCTPh)$_2$] (**Zn1**)	5.07	>88.8	22.6
PyC4ClPh	8.13	>119	18.9
HPyCT4ClPh (**2**)	9.96	>88.4	8.76
[Ga(PyCT4ClPh)$_2$]NO_3 (**Ga2**)	1.81	16.08	13.5
[Zn(PyCT4ClPh)$_2$] (**Zn2**)	4.74	>83.8	19.2
PyC4BrPh	6.19	>87.63	18.94
HPyCT4BrPh (**3**)	2.21	>68.51	19.55
[Ga(PyCT4BrPh)$_2$]NO_3 (**Ga3**)	0.96	28.85	14.36
[Zn(PyCT4BrPh)$_2$] (**Zn3**)	2.21	>60.5	>67.8
PyC4NO_2Ph	6.19	>100	12.8
HPyCT4NO_2Ph (**4**)	>74.1	>79.4	>157
[Ga(PyCT4NO_2Ph)$_2$]NO_3 (**Ga4**)	15.6	29.7	15.21
[Zn(PyCT4NO_2Ph)$_2$] (**Zn4**)	36.4	>74.5	>68.6
Thiosemicarbazide	565	4916	1742
Gallium nitrate	1802	997	>929
Zinc chloride	>1067	>2346	467
Tetracycline hydrochloride	0.37	7.31	–
Fluconazole	–	–	12.9

4. Conclusion

Chalcone-derived thiosemicarbazones were obtained, which present antibacterial and antifungal activities. In some cases, the thiosemicarbazones proved to be more potent as antimicrobial agents than the chalcone counterparts. Coordination of the thiosemicarbazones to zinc(II) resulted in activity improvement against *S. aureus,* but not against *C. albicans*. Coordination of the thiosemicarbazones to gallium(III) resulted in activity improvement against all studied micro-organisms. The thiosemicarbazones proved to be active against *gram*-positive *S. aureus* bacteria while their gallium(III) complexes were active against both *gram*-positive *S. aureus* and *gram*-negative *P. aeruginosa* strains. Hence, complexation to gallium(III) led to a broadening of the antibacterial spectrum of the studied thiosemicarbazones. Since gallium nitrate is inactive against all micro-organisms, coordination to the thiosemicarbazones resulted in significant improvement of gallium's antimicrobial profile.

The literature contains many reports on the antimicrobial properties of both chalcones [1] and thiosemicarbazones [3] and their metal complexes [39–43]. The preparation of chalcone-derived thiosemicarbazones and their zinc(II) and gallium(III) complexes revealed to be an effective strategy of obtaining potent antimicrobial agents which could constitute interesting drug candidate prototypes.

Supplementary data

CCDC 890760 contains the supplementary crystallographic data for this paper. These data can be obtained free of charge from The Cambridge Crystallographic Data Center via http://www.ccdc.cam.ac.uk/data_request/cif.

Acknowledgments

This work was supported by CNPq and INCT-INOFAR (Proc. CNPq 988573.364/2008-6) from Brazil.

References

[1] Z. Nowakowska. *Eur. J. Med. Chem.*, **42**, 125 (2007).
[2] M.L. Go, X. Wu, X.L. Liu. *Curr. Med. Chem.*, **12**, 483 (2005).
[3] H. Beraldo, D. Gambino. *Mini Rev. Med. Chem.*, **4**, 31 (2004).
[4] A.E. Liberta, D.X. West. *Biometals*, **5**, 121 (1992).
[5] I.C. Mendes, J.P. Moreira, A.S. Mangrich, S.P. Balena, B.L. Rodrigues, H. Beraldo. *Polyhedron*, **26**, 3263 (2007).
[6] J.G. Da Silva, L.S. Azzolini, S.M.S.V. Wardell, J.L. Wardell, H. Beraldo. *Polyhedron*, **28**, 2301 (2009).
[7] W.B. Júnior, M.S. Alexandre-Moreira, M.A. Alves, A. Perez-Reboleleo, G.L. Parrilha, E.E. Castellano, O.E. Piro, E.J. Barreiro, H. Beraldo. *Molecules*, **16**, 6902 (2011).
[8] J. Sheng, P.T.M. Nguyen, R.E. Marquis. *Arch. Oral Biol.*, **50**, 747 (2005).
[9] Y. Oyama, H. Matsui, M. Morimoto, Y. Sakanashi, Y. Nishimura, Y. Okano. *Toxicol. Lett.*, **171**, 138 (2007).
[10] P. Talukder, T. Satho, K. Irie, T. Sharmin, D. Hamady, Y. Nakashima, F. Miake. *Int. Immunopharmacol.*, **11**, 141 (2011).
[11] L.R. Bernstein. *Pharmacol. Rev.*, **50**, 665 (1998).
[12] J.A. Lessa, G.L. Parrilha, H. Beraldo. *Inorg. Chim. Acta*., **393**, 53 (2012).
[13] T.O. Bastos, B.M. Soares, P.S. Cisalpino, I.C. Mendes, R.G. dos Santos, H. Beraldo. *Microbiol. Res.*, **573**, 165 (2010).
[14] R.J. Martens, N.A. Miller, N.D. Cohen, J.R. Harrington, L.R. Bernstein. *J. Equine Vet. Sci.*, **27**, 341 (2007).
[15] Y. Kaneko, M. Thoendel, O. Olakanmi, B.E. Britigan, P.K. Singh. *J. Clin. Invest.*, **117**, 877 (2007).
[16] I.C. Mendes, M.A. Soares, R.G. Santos, C. Pinheiro, H. Beraldo. *Eur. J. Med. Chem.*, **44**, 1870 (2009).

[17] Oxford Diffraction. *CrysAlis PRO CCD and CrysAlis PRO RED: Version 1.171.33.55 (release 05 01 2010 CrysAlis171.NET)*, Oxford Diffraction Ltd., Yarnton, Oxfordshire, England (2010).
[18] G.M. Sheldrick. *Acta Cryst.*, **A64**, 112 (2008).
[19] V.V. Zakharychev, A.V. Kuzenkov. *Chem. Heterocycl. Comp.*, **43**, 989 (2007).
[20] L.J. Farrugia. *J. Appl. Cryst.*, **30**, 565 (1997).
[21] C.F. Macrae, I.J. Bruno, J.A. Chisholm, P.R. Edgington, P. McCabe, E. Pidcock, L. Rodriguez-Monge, R. Taylor, P.A. Wood. *J. Appl. Cryst.*, **41**, 466 (2008).
[22] L.J. Farrugia. *J. Appl. Cryst.*, **32**, 837 (1999).
[23] J. Pernak, J. Rogoza, I. Mirska. *Eur. J. Med. Chem.*, **36**, 313 (2001).
[24] National Committee for Clinical Laboratory Standards. *Methods for Dilution Antimicrobial Susceptibility Tests for Bacteria that Grow Aerobically; Approved Standard*, 6th Edn, NCCLS document M7-A6 (ISBN 1-56238-486-4). NCCLS, 940 West Valley Road, Suite 1400, Wayne, Pennsylvania 19087-1898, USA (2003).
[25] National Committee for Clinical Laboratory Standards. *Reference Method for Broth Dilution Antifungal Susceptibility Testing of Yeasts; Approved Standard*, 2nd Edn, NCCLS document M27-A2 [ISBN 1-56238-469-4]. NCCLS, Pennsylvania, USA (2002).
[26] M. Joseph, A. Sreekanth, V. Suni, M.R.P. Kurup. *Spectrochim. Acta A*, **64**, 637 (2006).
[27] K.S.O. Ferraz, N.F. Silva, J.G. Da Silva, N.L. Speziali, I.C. Mendes, H. Beraldo. *J. Mol. Struct.*, **1008**, 102 (2012).
[28] E.B. Seena, M.R.P. Kurup. *Spectrochim. Acta, Part A*, **69**, 726 (2008).
[29] I.C. Mendes, J.P. Moreira, N.L. Speziali, A.S. Mangrich, J.A. Takahashia, H. Beraldo. *J. Braz. Chem. Soc.*, **17**, 1571 (2006).
[30] P. Sengupta, R. Dinda, S. Ghosh. *Transition Met. Chem.*, **27**, 665 (2002).
[31] J.A. Lessa, J.C. Guerra, L.F. de Miranda, C.F.D. Romeiro, J.G. Da Silva, I.C. Mendes, N.L. Speziali, H. Beraldo. *J. Inorg. Biochem.*, **105**, 1729 (2011).
[32] A.P. Rebolledo, M. Vieites, D. Gambino, O.E. Piro, E.E. Castellano, C.L. Zani, E.M. Souza-Fagundes, L.R. Teixeira, H. Beraldo. *J. Inorg. Biochem.*, **99**, 698 (2005).
[33] K. Nakamoto. *Infrared and Raman Spectra of Inorganic and Coordination Compounds*, 4th Edn, p. 254, John Wiley and Sons, New York, NY (1986).
[34] A.P. Rebolledo, G.M. de Lima, L.N. Gambi, N.L. Speziali, D.F. Maia, C.B. Pinheiro, J.D. Ardisson, H. Beraldo. *Appl. Organomet. Chem.*, **17**, 945 (2003).
[35] J.G. Da Silva, S.M.S.V. Wardell, J.L. Wardell, H. Beraldo. *J. Coord. Chem.*, **62**, 1400 (2009).
[36] O.E. Offiong. *Spectrochim. Acta, Part A*, **50**, 2167 (1994).
[37] O.M.I. Adlly. *Spectrochim. Acta, Part A*, **79**, 1295 (2011).
[38] J.S. Casas, E.E. Castellano, J. Ellena, M.S.G. Tasende, A. Sánchez, M.J. Vidarte. *Inorg. Chem.*, **42**, 2584 (2003).
[39] U. El-Ayann. *J. Coord. Chem.*, **65**, 629 (2012).
[40] N.V. Savawant, J.B. Biswal, S.S. Garje. *J. Coord. Chem.*, **64**, 1758 (2011).
[41] M. Muthukumar, P. Viswanathamurthi. *J. Coord. Chem.*, **63**, 1263 (2010).
[42] S. Sumathi, P. Tharmaraj, C.D. Sheela, R. Ebenezer. *J. Coord. Chem.*, **64**, 1707 (2011).
[43] S. Sumathi, P. Tharmaraj, C.D. Shella, R. Ebenezer, P.S. Bhava. *J. Coord. Chem.*, **64**, 1673 (2011).